Supporting Information

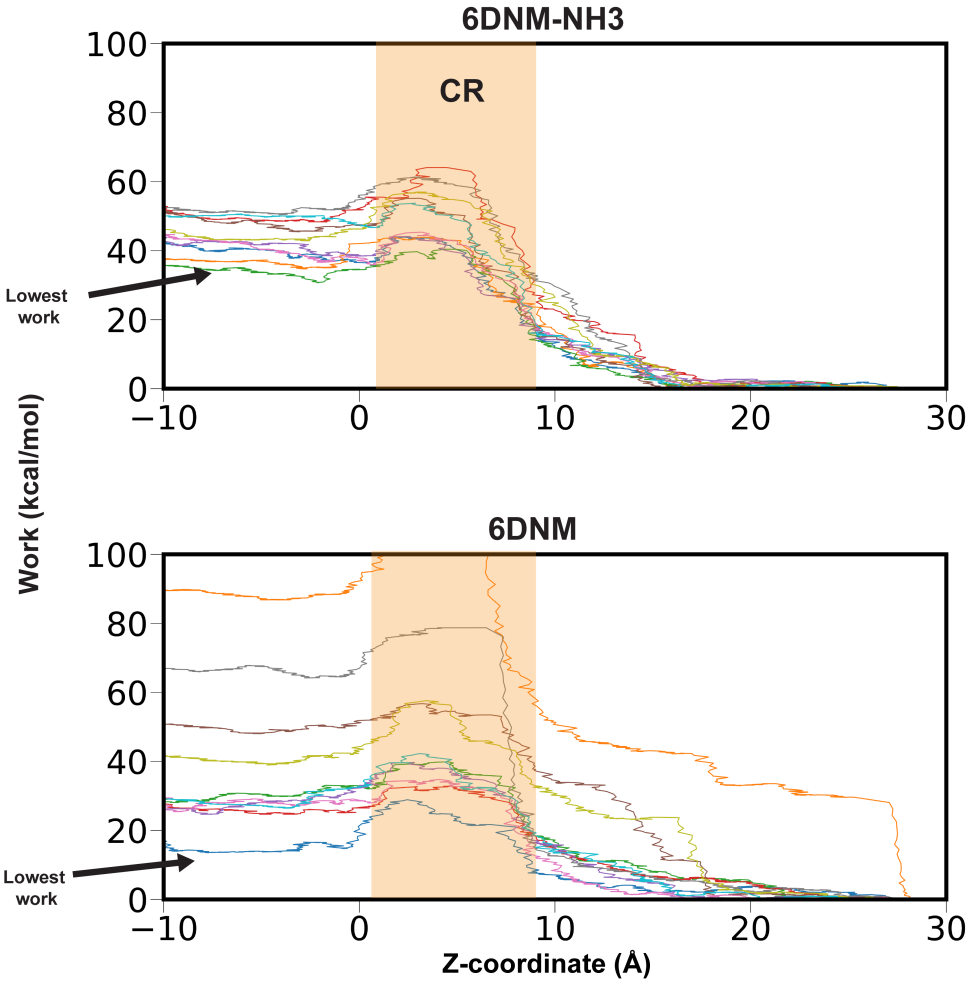

Figure S1: The accumulated non-equilibrium work during different independent SMD simulations (represented in unique color) of 6DNM-NH3 (*top*) and 6DNM (*bottom*). Work values are projected onto the position of the drug along the membrane normal (z-axis) and relative to the midplane of the membrane ($z = 0$). The location of the CR is highlighted in orange.

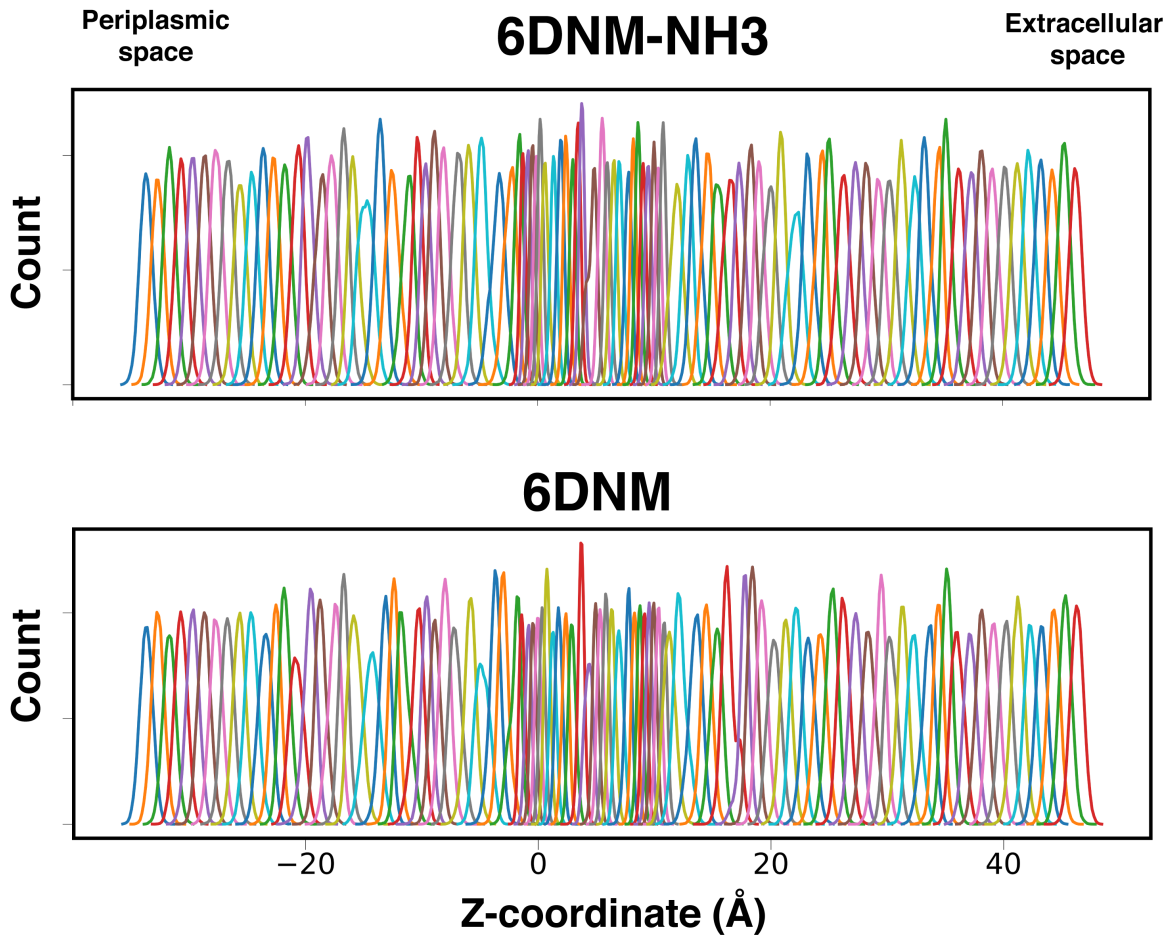

Figure S2: Window overlaps from SMD-seeded BEUS simulations for permeation of 6DNM-NH3 (*top*) and 6DNM (*bottom*) through OmpF. The histograms show distribution probabilities of the drug along the membrane normal (Z-axis) in each replica (window). Windows are spaced at 1 Å intervals for a span of 80 Å extending from the periplasmic ($Z = -34$ Å) to the extracellular bulk solution ($Z = 46$ Å), except for the region between the entrance and exit of the CR ($Z = -3$ to 12 Å) where a 0.5-Å spacing was used to ensure adequate histogram overlap.

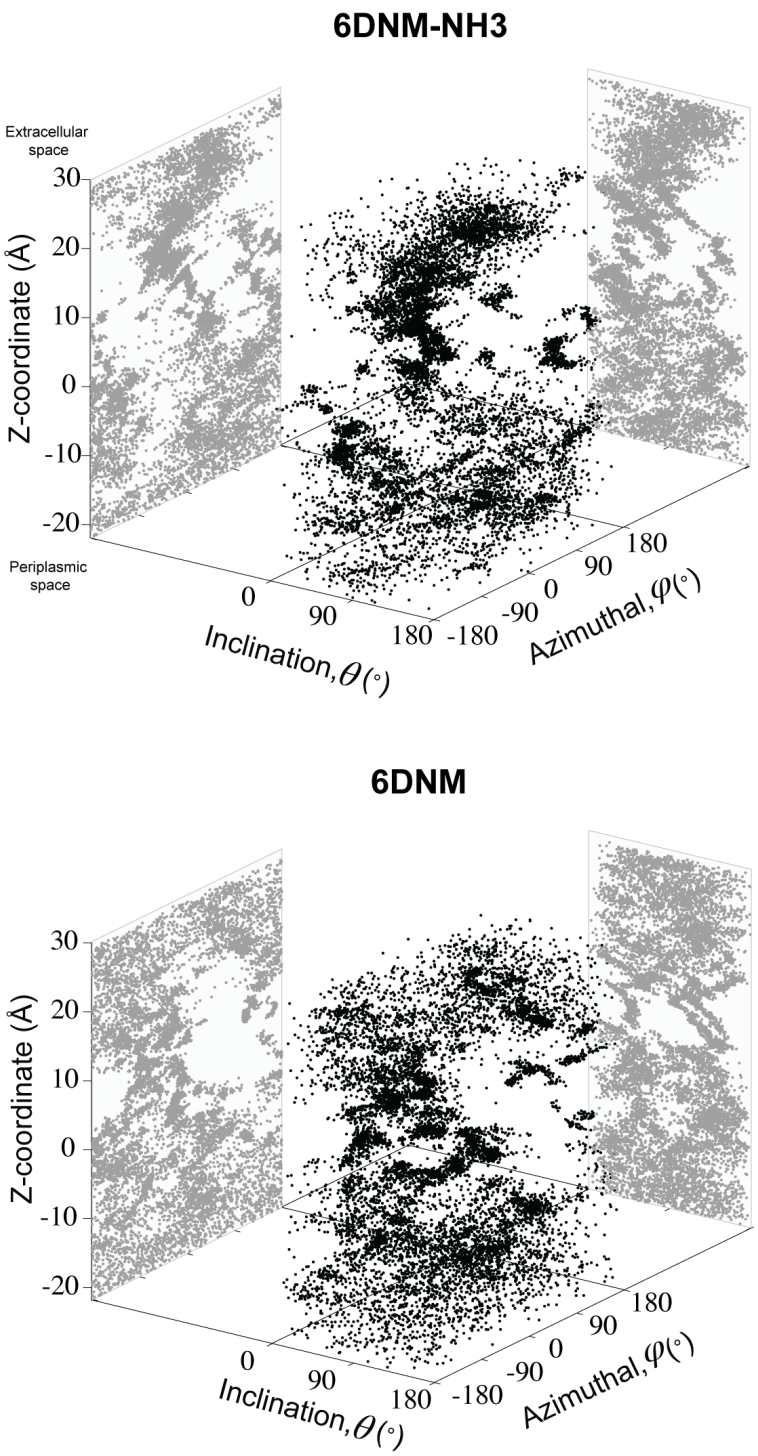

Figure S3: Sampling of 6DNM-NH3 (*top*) and 6DNM (*bottom*) during their respective 10 independent SMD simulations projected on the orientation (inclination and azimuthal) and translation (Z-coordinate) DOFs of the antibiotic.

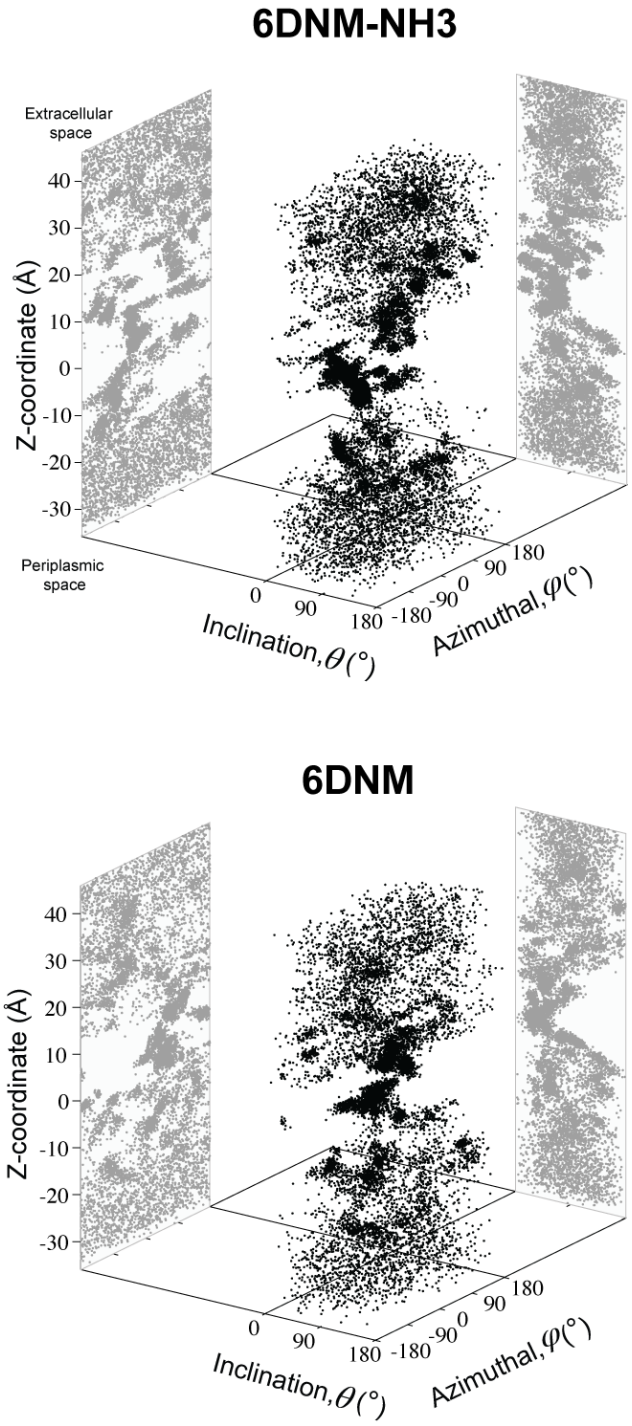

Figure S4: Sampling of 6DNM-NH3 (*top*) and 6DNM (*bottom*) during their respective SMD-seeded BEUS simulations projected on the orientation (inclination and azimuthal) and translation (Z-coordinate) DOFs of the antibiotic.

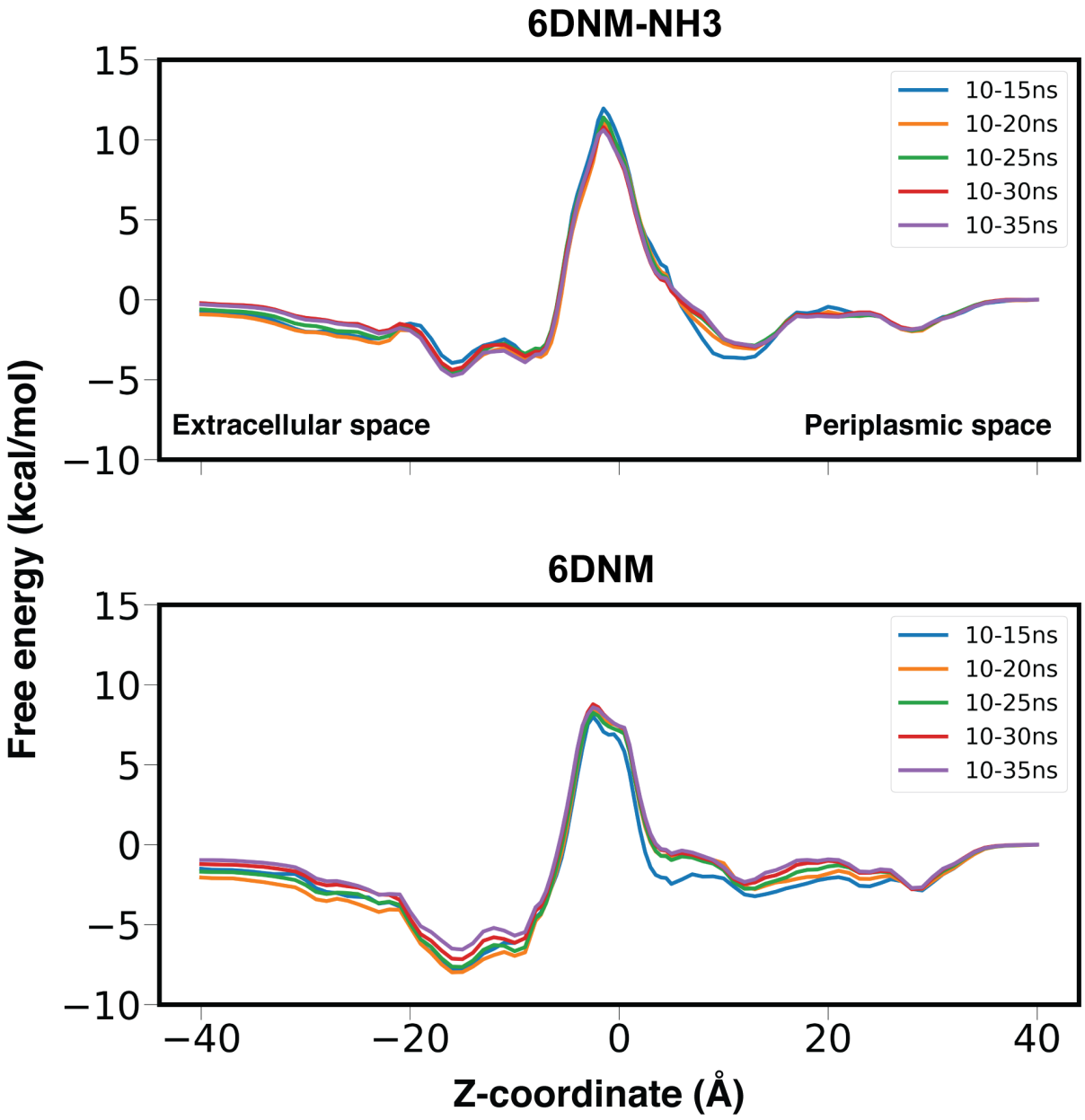

Figure S5: Convergence of potential of mean force (PMF) calculations derived from SMD-seeded BEUS was monitored by calculating permeation free energy for 6DNM-NH3 (*top*) and 6DNM (*bottom*) for different simulation segments in each BEUS window after discarding the first 10 ns (10–15 ns, 10–20 ns, 10–25 ns, 10–30 ns, and 10–35 ns). Free energies are projected onto the Z-coordinate of the C.O.M of each drug.

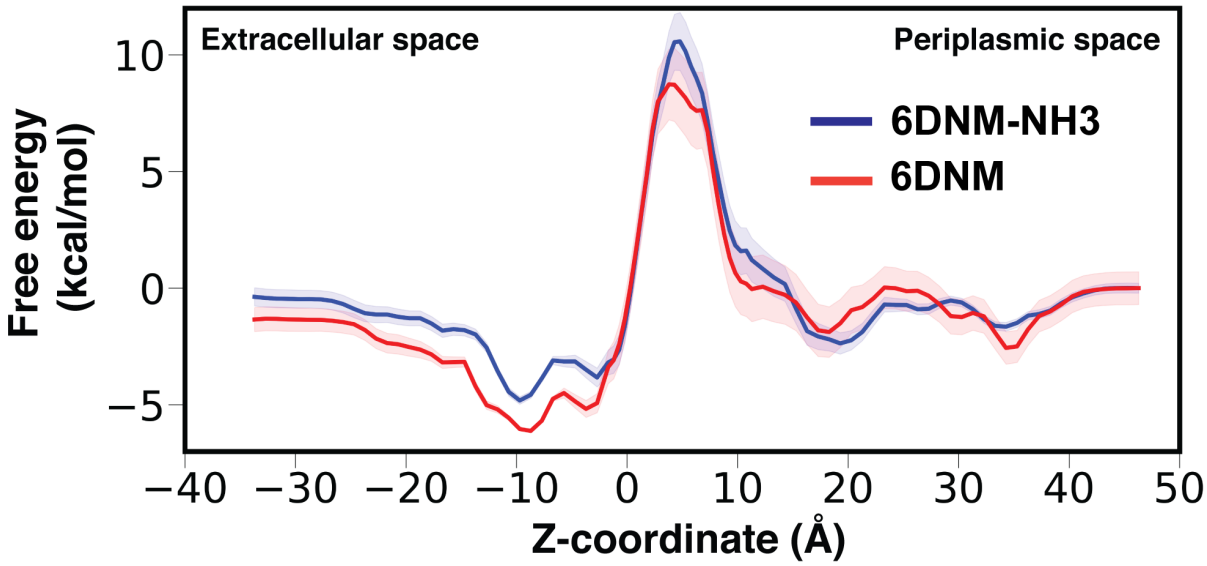

Figure S6: Mean (solid) and standard deviation (shaded) of the free energy values for the permeation of 6DNM-NH3 (blue) and 6DNM (red), calculated using all the SMD-seeded BEUS windows, projected along the Z-coordinate of the antibiotic C.O.M.

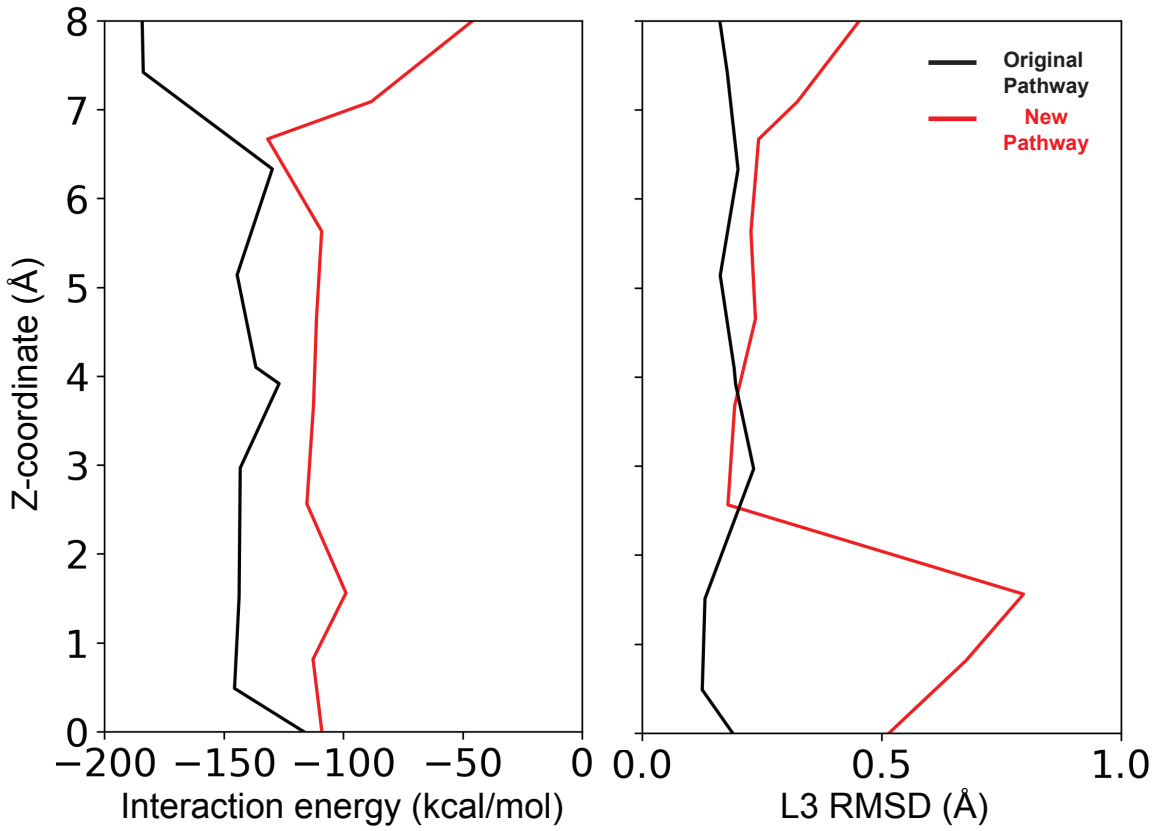

Figure S7: Comparison of drug-protein interaction energies (*left*) and L3 RMSD (*right*) along the Z-coordinate of 6DNM-NH3 for the original (black) and new pathway determined without restraining protein backbone (red).

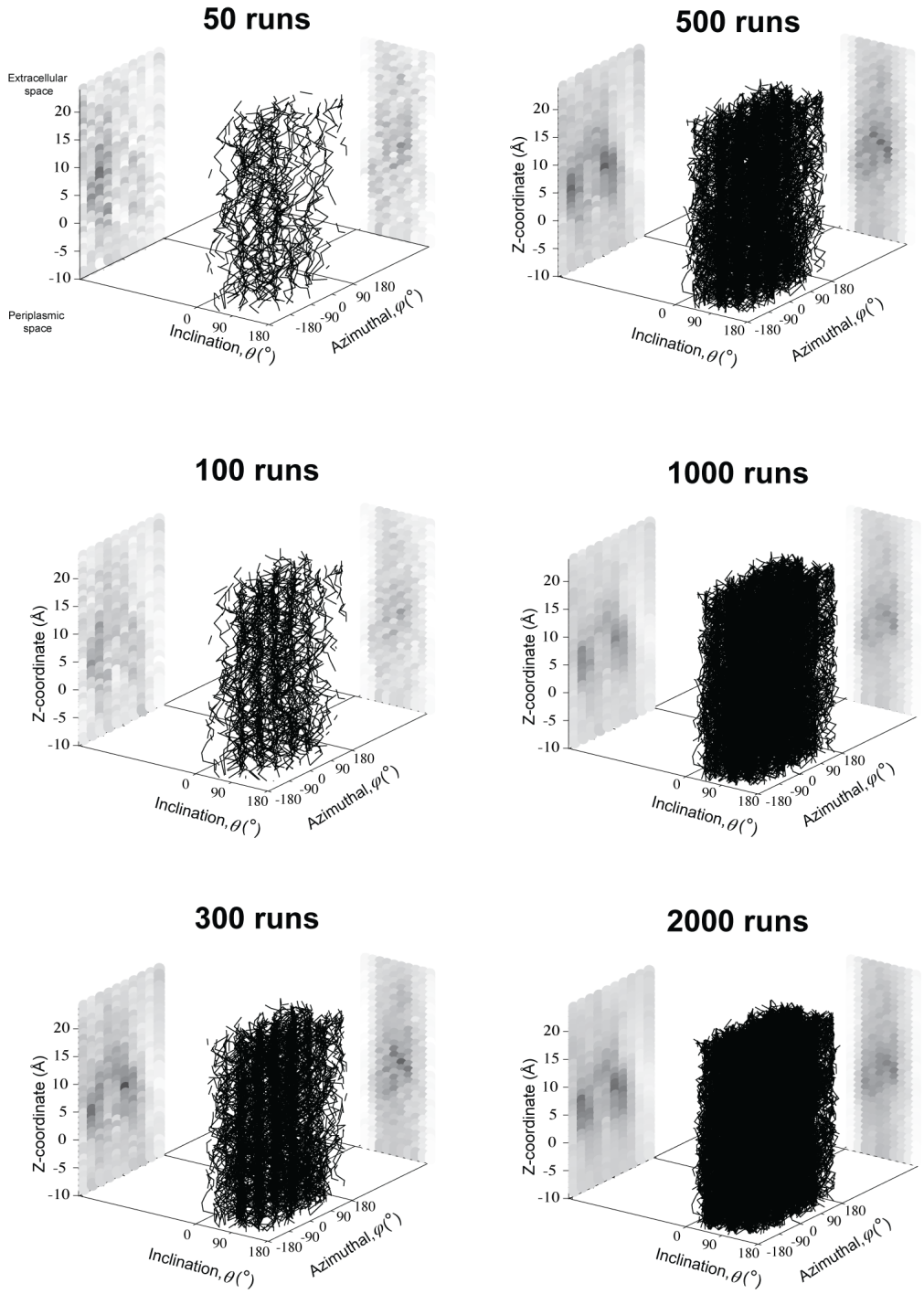

Figure S8: Convergence of MCPS runs of 6DNM-NH3, determined by projecting the Boltzmann weighted densities of the MCPS trajectories at different numbers of runs along the Z-coordinate, inclination (θ) and azimuthal (ϕ) of the antibiotic.

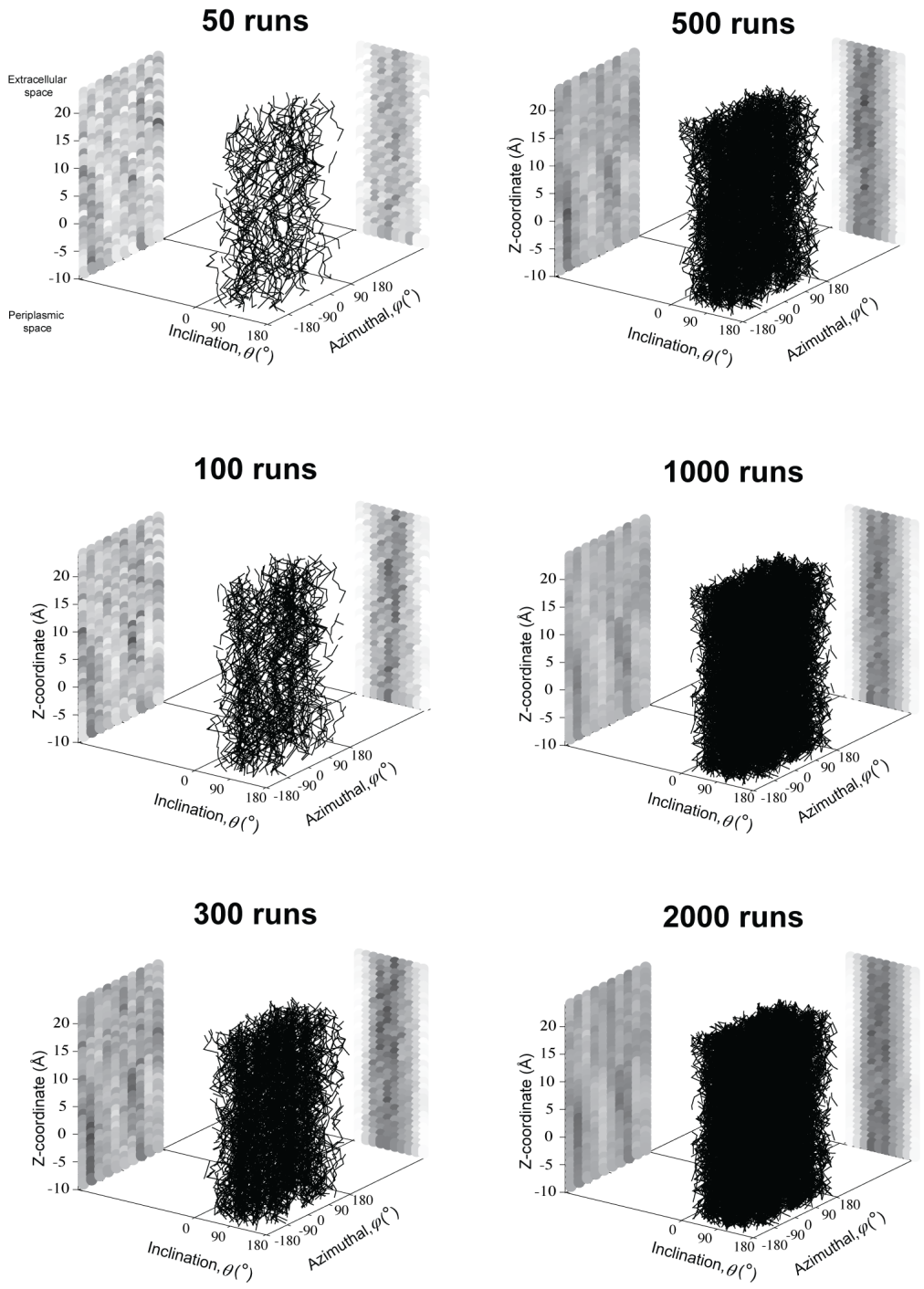

Figure S9: Convergence of MCPS runs of 6DNM, determined by projecting the Boltzmann weighted densities of the MCPS trajectories at different number of runs along the Z-coordinate, inclination (θ) and azimuthal (ϕ) of the antibiotic.

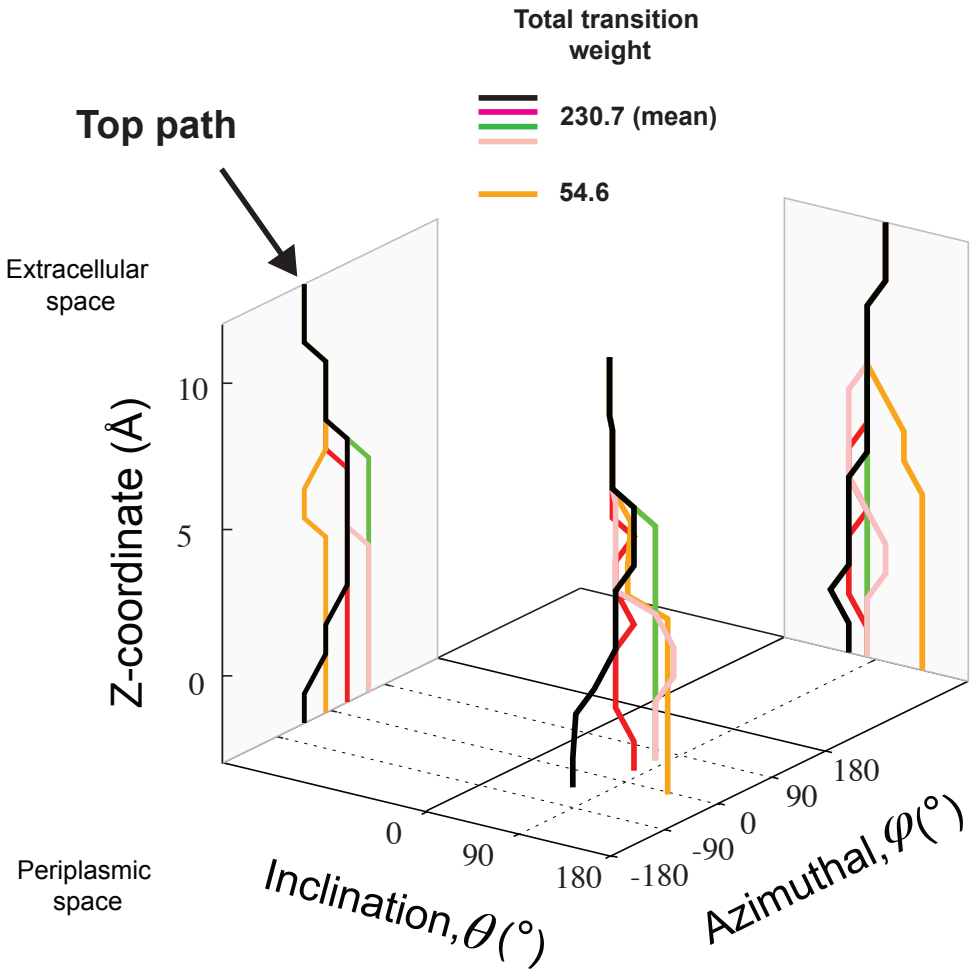

Figure S10: Top 5 permeation pathways for 6DNM-NH3. The pathways are categorized into two groups based on their similarities in the configurational space: orange represents one and other colors represent the other group of pathways. Black is the top pathway. The total transition weight of each path is the sum of the transitions along the edges of the path.

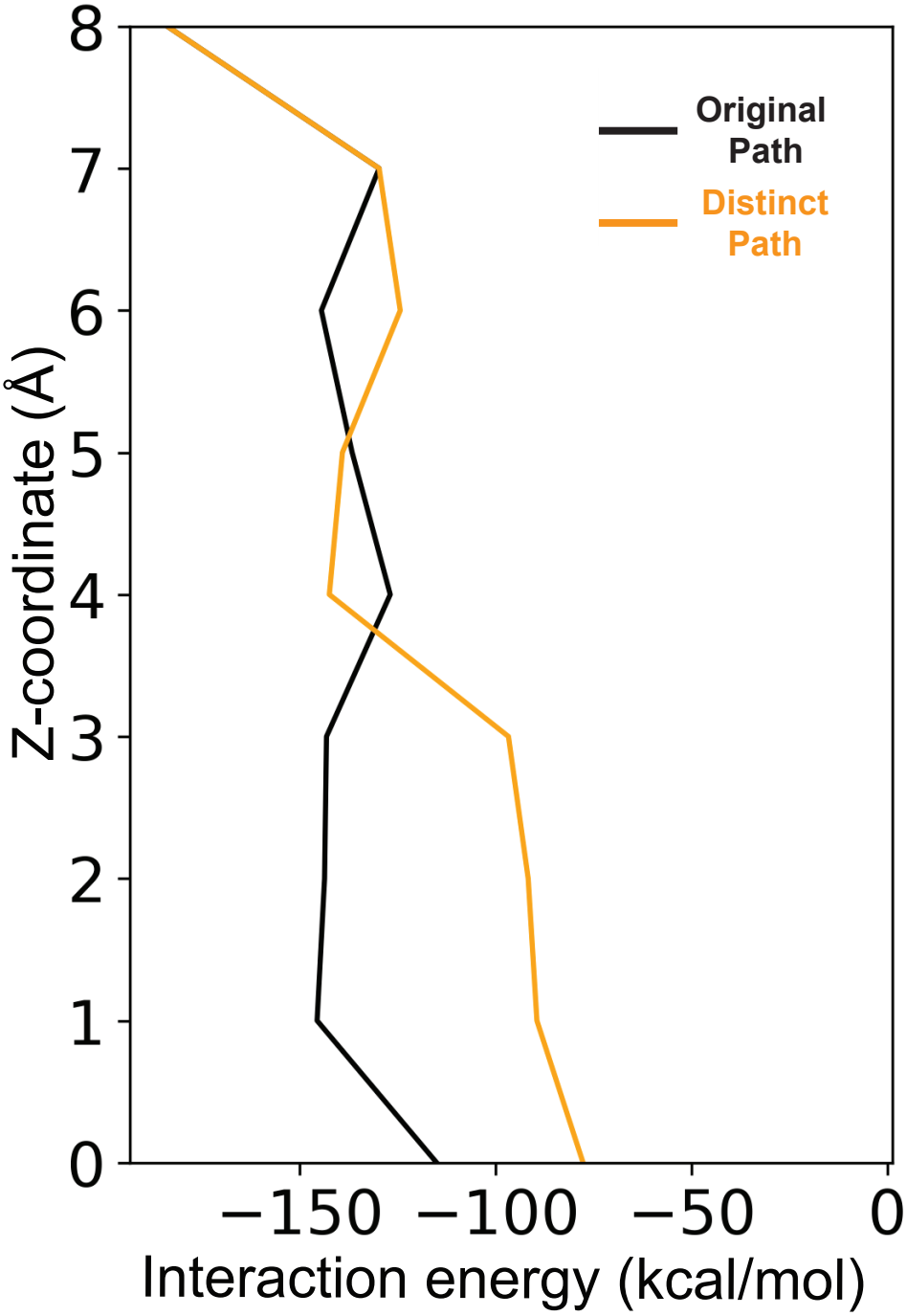

Figure S11: The drug-protein interaction energies for 6DNM-NH3 for the original (black) and new distinct pathway (orange) along the Z-coordinate of the C.O.M of the drug.

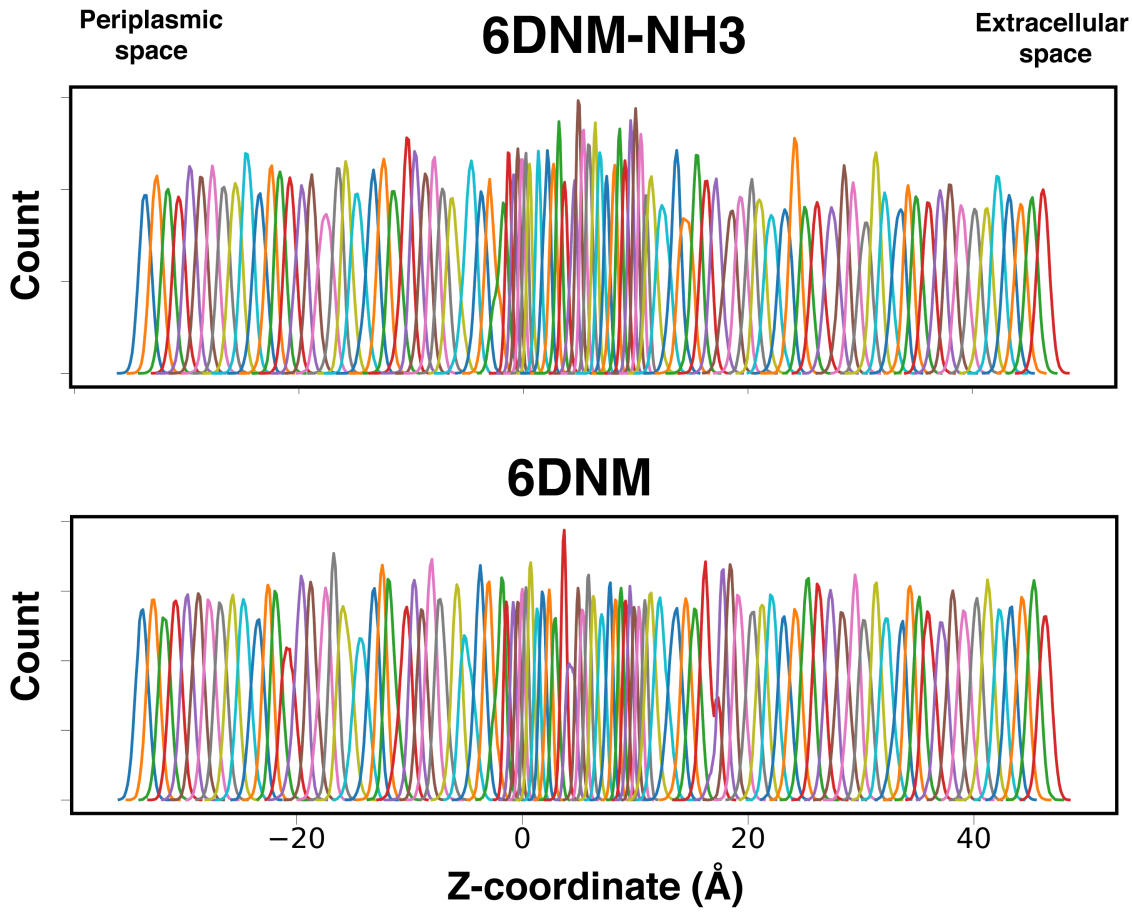

Figure S12: Window overlaps from MCPS-seeded BEUS simulations for permeation of 6DNM-NH3 (*top*) and 6DNM (*bottom*) through OmpF. The histograms show distribution probabilities of the drug along the membrane normal (Z-axis) in each replica (window). Windows are spaced at 1 Å intervals for a span of 80 Å extending from the periplasmic ($Z = -34$ Å) to the extracellular bulk solution ($Z = 46$ Å), except for the region between the entrance and exit of the CR ($Z = -3$ to 12 Å) where a 0.5-Å spacing was used to ensure adequate histogram overlap.

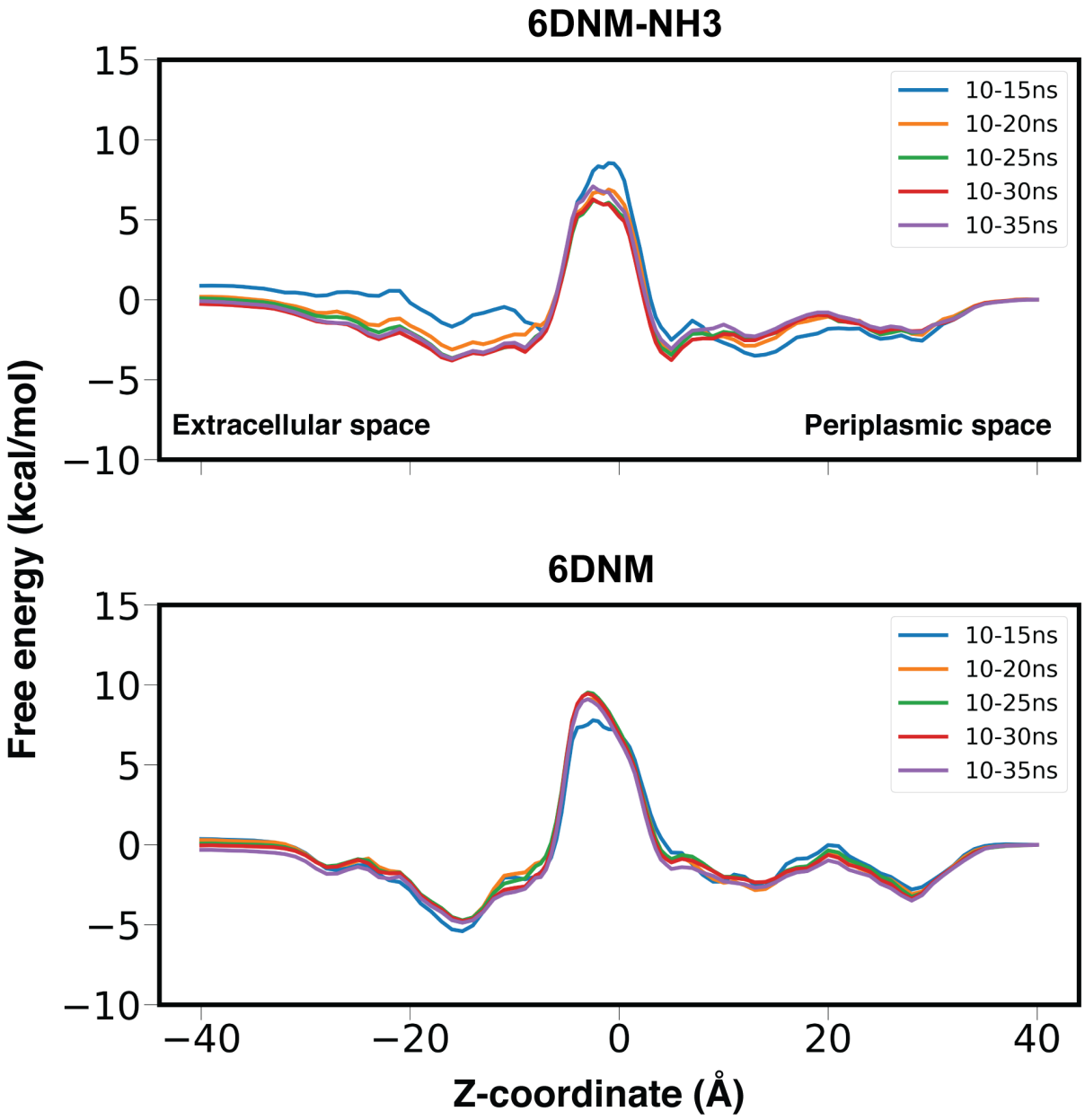

Figure S13: Convergence of PMF calculations for MCPS-seeded BEUS simulations was monitored by calculating permeation free energy for 6DNM-NH3 (*top*) and 6DNM (*bottom*) at different simulation times in each BEUS window after discarding the first 10 ns (10–15 ns, 10–20 ns, 10–25 ns, 10–30 ns, and 10–35 ns). Free energies are projected onto the Z-coordinate of the C.O.M of the drug.

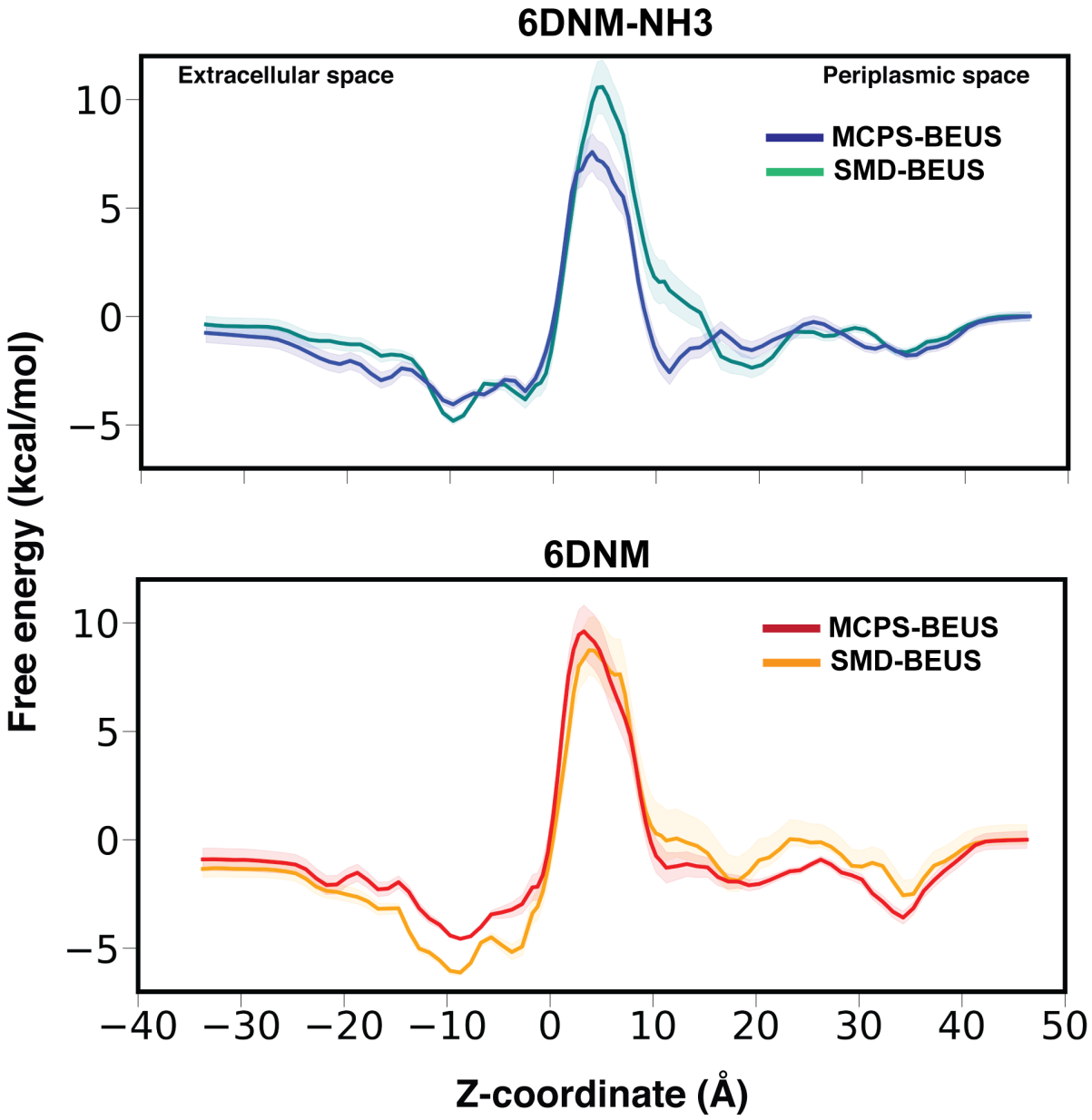

Figure S14: Comparison of free energy of permeation derived from SMD-seeded BEUS and MCPS-seeded BEUS simulations for 6DNM-NH3 (*top*) and 6DNM (*bottom*). For 6DNM-NH3, a significant decrease (by ≈3 kcal/mol) in the energetic barrier is observed in the free energy profile derived using MCPS-seeded BEUS than the one derived from SMD-seeded BEUS. For 6DNM, the barrier remains similar in both approaches.

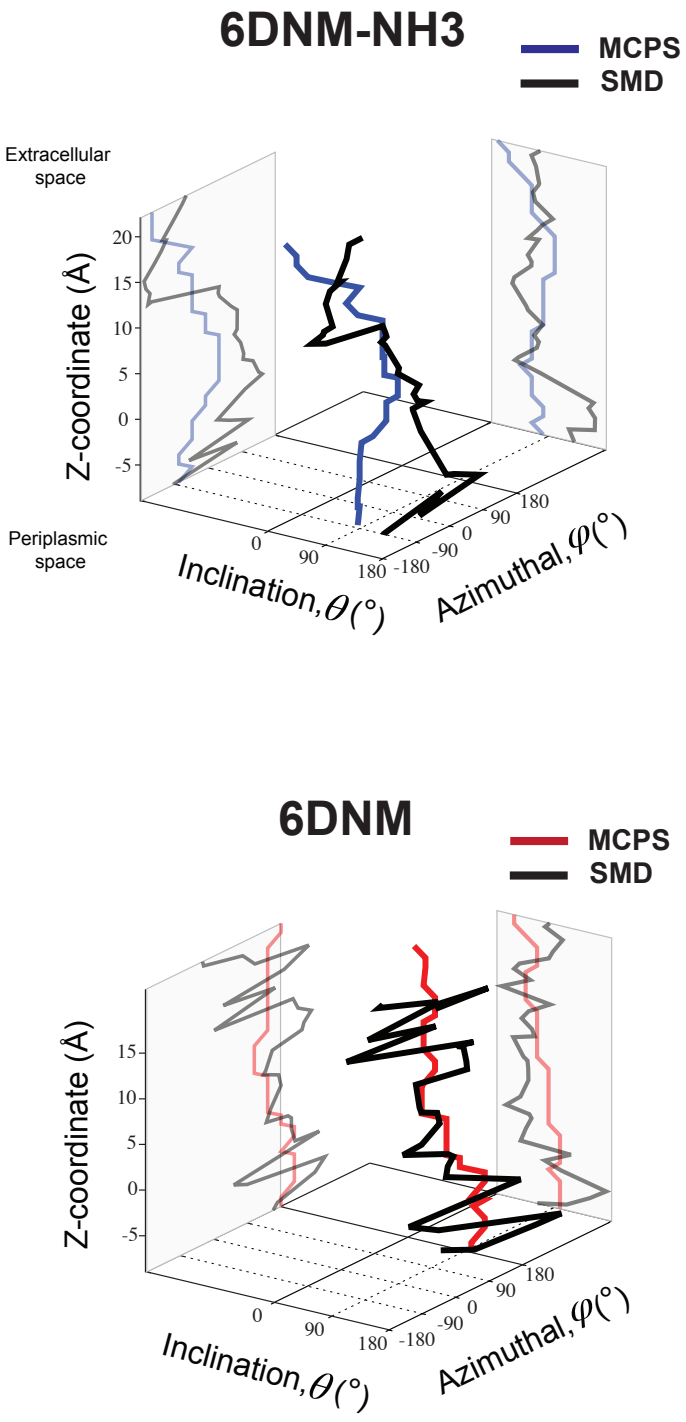

Figure S15: Comparison of the initial permeation pathways derived using MCPS and SMD for 6DNM-NH3 (*top, blue*) and 6DNM (*bottom, red*) through OmpF. Pathways are projected onto the orientation (inclination and azimuthal) and Z-coordinate of the antibiotic. These pathways were used to seed the BEUS simulations.

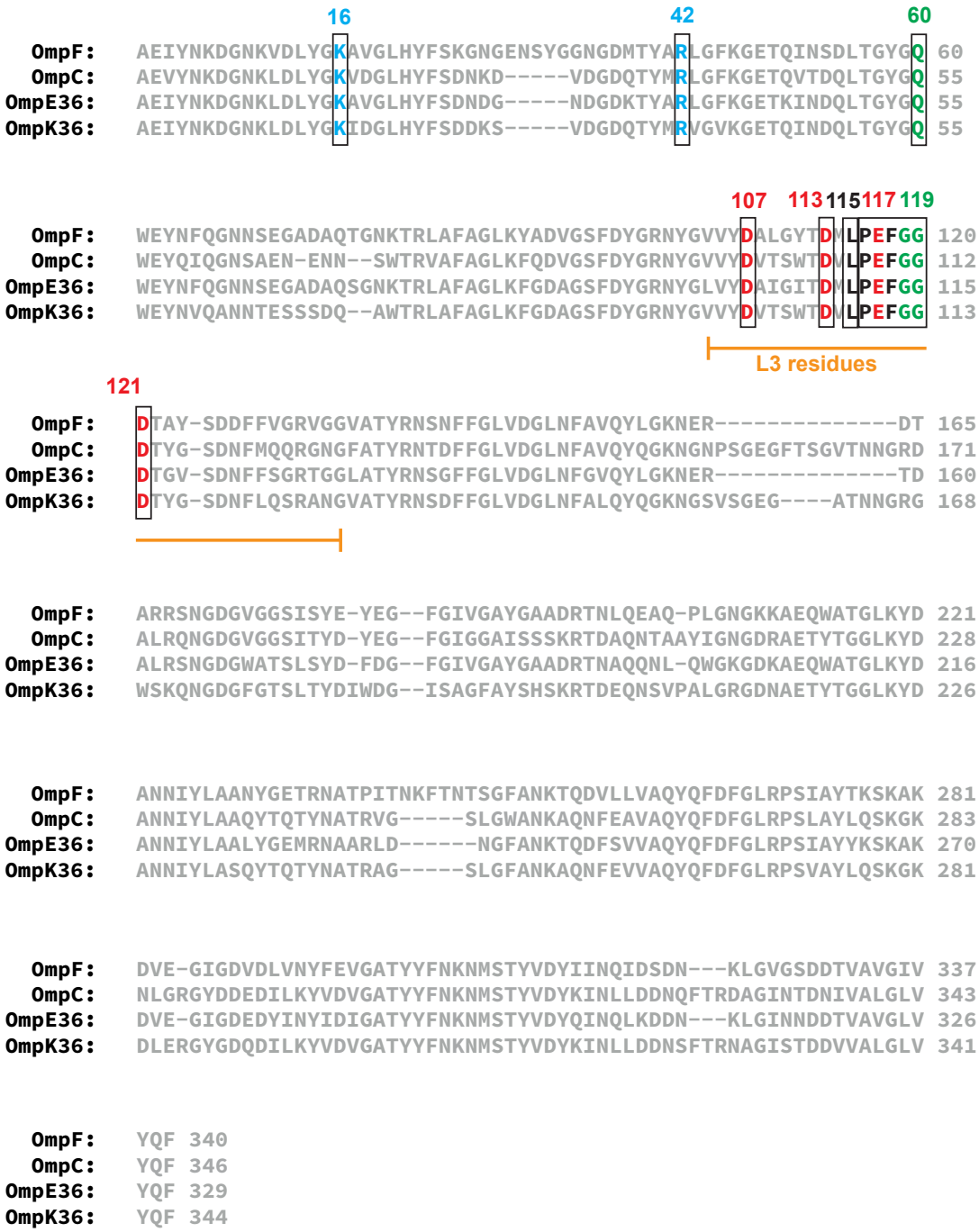

Figure S16: Sequence alignment of OmpF (*E. coli*), OmpC (*E. coli*), OmpK36 (*K. pneumoniae*) and OmpE36 (*E. cloacae*). Each residue is represented by their one-letter code. Important residues in the observed permeation mechanism through OmpF are highlighted with a box and colored based on residue type (black: hydrophobic, green: polar, red: acidic, and blue: basic). All other residues are colored gray. The alignment was performed on full-length sequences using the Clustal Omega[94] alignment tool within Uniprot.[95]